JOURNAL OF MOLECULAR SPECTROSCOPY 125, 274–287 (1987)

Accurate Rotational Constants of CO, HCl, and HF: Spectral Standards for the 0.3- to 6-THz (10- to 200-cm^{-1}) Region

I. G. NOLT[1] AND J. V. RADOSTITZ

Department of Physics, University of Oregon, Eugene, Oregon 97403

G. DILONARDO

Dipartimento di Chimica Fisica ed Inorganica, Università di Bologna, 40136 Bologna, Italy

K. M. EVENSON, D. A. JENNINGS, K. R. LEOPOLD,[2] M. D. VANEK, AND L. R. ZINK[3]

Time and Frequency Division, National Bureau of Standards, Boulder, Colorado 80303

A. HINZ[4]

Institut for Angewandte Physik, Universitat Bonn, D-5300 Bonn 1, Federal Republic of Germany

AND

K. V. CHANCE

Harvard-Smithsonian Center for Astrophysics, Cambridge, Massachusetts 02138

Accurate high-resolution spectroscopic measurements require secondary standards which can serve as convenient calibration references in laboratory and field research. We have measured the frequencies of a series of rotational transitions between 0.3 and 6 THz for several stable and readily obtainable gases (CO, HCl, and HF) to an accuracy better than one part in 10^7 and present revised rotational constants for these molecules. The gases were selected (in part) due to their presence in the Earth's atmosphere in significant amounts and thus are convenient for the frequency calibration of atmospheric spectra.

I. INTRODUCTION

Progress in submillimeter and far-infrared (FIR) spectroscopy has led to an increasing amount of high-resolution wavelength-based (interferometric) spectroscopic research for which the accuracy of available spectral references is only marginally adequate.

[1] Present address: Environmental Sensors Branch, Code 474, NASA Langley, Hampton, VA 23665.

[2] National Research Council Postdoctoral Research Fellow. Present address: Chemistry Department, University of Minnesota, Minneapolis, MI 55455.

[3] Present address: Physical Chemistry Laboratory, South Parks Road, Oxford OX1 3QZ, England.

[4] Present address: Carl Zeiss, SOE-2, Postfach 1369/1380, D-7082 Oberkochen, Federal Republic of Germany.

0022-2852/87 $3.00

Harmonic generation from high-frequency microwave sources can provide precision frequency measurements in the frequency range up to about 1 THz (*1*). Calibration frequencies in the FIR above 1 THz, which rely on molecular frequencies obtained by fitting rotational transitions measured from harmonics of microwave sources (*2*), become increasingly inaccurate in the extrapolation to higher frequencies due to centrifugal distortion. Specifically, Fourier transform spectroscopy (FTS) is used to provide broad frequency coverage in the FIR, but it is necessary for the highest accuracy to refer these FTS measurements to secondary molecular frequency standards.[5] This latter approach is illustrated in the recent work of Johns (*3*), who, by using some preliminary measurements of this study, achieved a spectral modeling of H_2O to a one-sigma uncertainty of 0.0002 cm^{-1} (6 MHz).

Our objective in this study is to provide a comprehensive set of secondary frequency references for the FIR using the tunable, laser-derived FIR radiation techniques developed by the Time and Frequency Division of the National Bureau of Standards (*4*). These new techniques for producing tunable far-infrared radiation provide about two orders of magnitude less uncertainty than high-resolution FTS methods (*3*). There is an important distinction between the two approaches. For the case of FTS measurements, instrumental resolution is the principal factor limiting frequency accuracy. For tunable radiation spectroscopy in which the line profile is fully resolved, the frequency accuracy is limited by the Doppler linewidth and other factors, as discussed in the following section.

II. EXPERIMENTAL DETAILS

We used two different techniques to generate FIR radiation of high spectral purity. In the first method,

$$\nu_{\mathrm{FIR}} = \nu_{\mathrm{I}} - \nu_{\mathrm{II}}, \tag{1}$$

where ν_{I} is the frequency[6] of a stabilized single-mode CO_2 laser, and ν_{II} is the frequency of a tunable CO_2 waveguide laser which is referred to a third stabilized single-mode CO_2 laser for its frequency control. This method was first described by Peterson *et al.* (*4*) and is illustrated schematically in Fig. 1. Here the mixing is second order (two wave) in a metal–insulator–metal (MIM) diode, and the FIR frequency is the frequency difference of the two CO_2 lasers which are incident on the MIM diode.

Our second method employed third-order (three wave) mixing, and the relevant schematic diagram is shown in Fig. 2. Here two fixed frequency stabilized CO_2 lasers, operating at frequencies[6] ν_{I} and ν_{II}, and a tunable microwave component at frequency ν_μ all have their radiation coupled on a MIM diode. The three frequencies are combined to produce a FIR frequency in this case given by

$$\nu_{\mathrm{FIR}} = (\nu_{\mathrm{I}} - \nu_{\mathrm{II}}) \pm \nu_\mu. \tag{2}$$

[5] The 1983 redefinition of the meter (*Comptes Rendus des Séances de la 17^e* CGPM, BIPM, Sevres, France, 1983) fixes the value of c and defines the meter as follows, "The meter is the length of the path travelled by light in vacuum during a time interval of 1/299 792 458ths of a second." This definition serves to provide a single, common standard for frequency and wavelength.

[6] In some measurements, the use of an acousto-optic modulator introduced a small frequency shift (typically 90 MHz) to the CO_2 frequency incident on the mixing diode. See Figs. 1 and 2.

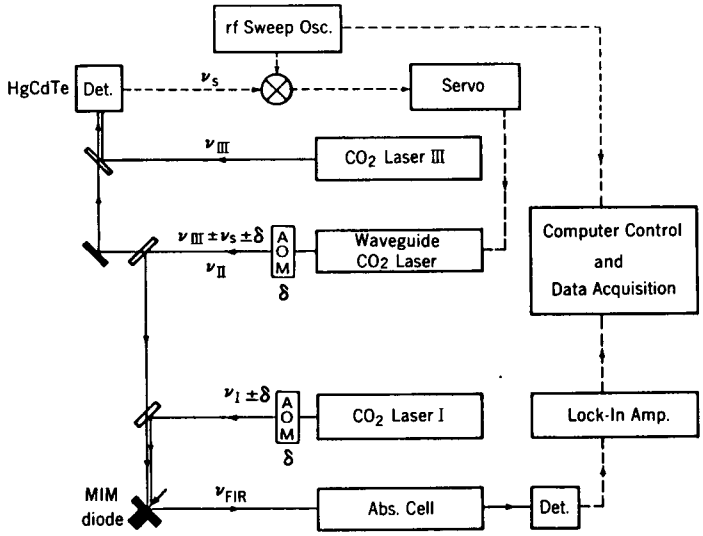

FIG. 1. Tunable FIR spectrometer which uses a waveguide laser for the tunable frequency component. This system corresponds to two wave or second-order mixing. The acousto-optic modulator (AOM) shifts the laser frequency by $\pm\delta$, and reduces the level of feedback-excited power fluctuations of the CO_2 laser. The frequency ν_s is an rf offset frequency.

A microwave sweeper provides up to ±20 GHz tunability, where one of the microwave sidebands is selected to sweep the spectral region of interest. However, the advantage of broad tunability is somewhat offset because third order has lower FIR power than second-order mixing.

In both systems the metal–insulator–metal diode is a 25-μm diameter, pointed tungsten wire contacting the polished end of a metal substrate at normal incidence.

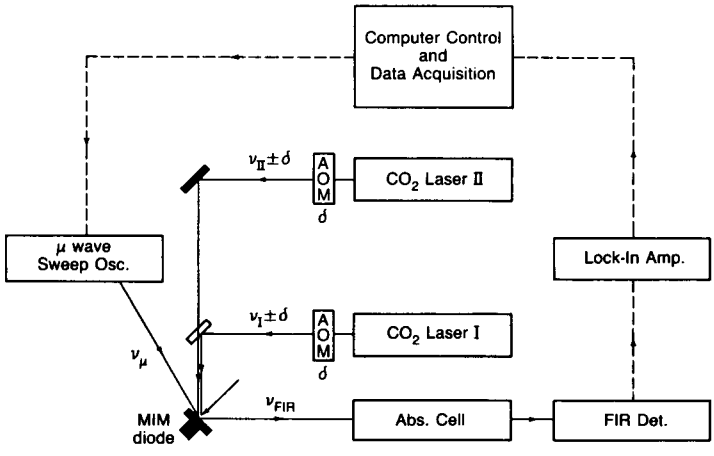

FIG. 2. Tunable FIR spectrometer which uses an rf frequency synthesizer for the tunable frequency component. This system corresponds to three wave or third-order mixing.

The properties of this contact with the metal post provide the nonlinear current-voltage characteristic which generates the FIR radiation. The tungsten wire of several millimeter length functions as a long wire antenna for the FIR radiation. The FIR radiated power is reflected by a section of a parabolic reflector and propagated along the axis of a single-pass Pyrex absorption cell (10- to 50-cm long and 19-mm inside diameter). The cell has high density polyethylene windows, and the transmitted power is sensed by an appropriate detector. The amount of FIR power at the detector depends upon several variables. To prevent diode damage, the total CO_2 power at the MIM diode is generally limited to about 200 mW; in second order, this results in 100 to 500 nW of FIR radiation. In third order, the FIR power is typically one-third of this amount.

The optimization of the diode junction remains poorly understood and is largely a matter of experimental practice. Our best junctions for second-order operation use nickel bases. For third order we have less experience, but contacts to cobalt substrates are better than those to nickel. Considerable patience is required, especially in third order, as the whisker contact needs careful and repeated adjustment to maximize the FIR power.

The FIR radiation is frequency modulated at a 1-kHz rate with a typical amplitude of 2.5 MHz by application of an ac voltage to the piezoelectric transducer frequency stabilization control of one of the CO_2 lasers. The modulated FIR frequency is scanned across the spectral region of interest by one of the two techniques described previously, and the resulting FIR signal is the modulation-broadened first derivative of the absorption as a function of frequency. The baseline signal crossing position indicates the absorption line center frequency and the absolute maxima of this signal correspond to the inflection positions of the absorption profile. A measured spectrum using third-order mixing is shown in Fig. 3.

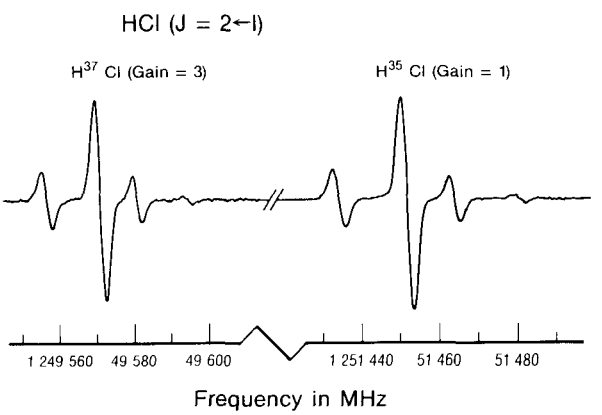

FIG. 3. Measurement of the $J = 2 \leftarrow 1$ transition of HCl illustrating the wide scanning capability of the third-order spectrometer. In this case eight HFS transitions for each isotope are seen as four features whose spectroscopic compositions are given in Tables III–VI. For this measurement we used a pumped ^{4}He-cooled germanium bolometer and preamp system which was engineered for optimum response at the signal modulation of 1 kHz. The scan for each isotope is an average of two frequency scans over the indicated ranges in a total time of 3.5 min.

The signal-to-noise ratio of the absorption profile depends upon several factors. The FIR power varies with each contact of the diode, and the noise due to the FIR power fluctuations is often greater than the intrinsic detector noise, although, some recent refinements have improved the overall performance. First, acousto-optic couplers have been added to isolate the CO_2 lasers from the diode. This isolation serves to reduce power fluctuations in the CO_2 laser caused by feedback. Second, detector systems have been optimized for phase-sensitive detection of the FIR at a modulation frequency of 1 kHz, which is a reasonable trade off between $1/f$ signal noise and detector responsivity. With the best second-order diodes, the laser driven FIR intensity fluctuations exceed the detector noise; however, in third order, overall noise is dominated by detector noise because the FIR power is less. In addition to the detector noise on the signal, the crossing point can also be perturbed by transient power changes and standing wave effects between the diode and the detector. The latter effects are suppressed in part by mounting all optical transmission elements (windows, filters, detectors) at small angles from normal incidence to the radiation direction.

The uncertainty in the measurement of a line center position is 0.1 to 0.2 MHz

TABLE I

Data Set for CO (MHz)

J'-J"	This Study	Microwave	Selected Value[a] for fit
1-0	--	115 271.204(10)[b]	
		115 271.195(30)[c]	115 271.204(10)
2-1	--	230 537.974(60)[c]	230 537.974(60)
3-2	--	345 795.900(180)[c]	
		345 795.989(64)[d]	345 795.989(64)
4-3	--	461 040.811(64)[d]	461 040.811(64)
5-4	576 267.910(72)	576 267.934(64)[d]	576 267.922(64)
6-5	--	691 472.978(64)[d]	691 472.978(64)
7-6	806 651.776(80)	--	806 651.776(80)
15-14	1 726 602.470(78)	--	1 726 602.470(78)
20-19	2 299 569.690(92)	--	2 299 569.690(92)
24-23	2 756 387.579(94)	--	2 756 387.579(94)
27-26	3 097 909.360(90)	--	3 097 909.360(90)
34-33	3 890 442.903(140)	--	3 890 442.903(140)

(a) The 2σ uncertainty shown in parentheses applies to last digits.
(b) Ref. 8.
(c) Ref. 9.
(d) Ref. 10. We estimated a 2σ uncertainty (95% confidence limits) of ±64 kHz from the residuals of their fit.

under conditions which give good signal-to-noise ratios. This uncertainty must be combined with the uncertainty of the FIR frequency, which is the combined quadratic sum (typically 35 kHz) of the uncertainties of the two CO_2 laser line frequencies. The 35-kHz uncertainty reflects the realization of CO_2 frequencies (5) using our saturated absorption stabilized lasers. Only in case of the strongest, narrowest lines was the line center measured with sufficient accuracy that the underlying uncertainty of the FIR frequency affected the accuracy of the final measurement.

In the following sections we discuss the measurements and analysis for each molecule, including the calculated frequencies for all the transitions over our measured range using the derived parameters.

TABLE II

Observed and Calculated CO Rotational Frequencies[a]

	Calculated Frequency in:		
J'-J"	cm^{-1}	MHz	Obs-calc (MHz)
1- 0	3.845 033 3	115 271.20	0.00
2- 1	7.689 919 7	230 538.00	-0.03
3- 2	11.534 512	345 795.98	0.01
4- 3	15.378 664	461 040.75	0.06
5- 4	19.222 228	576 267.91	0.01
6- 5	23.065 058	691 473.05	-0.07
7- 6	26.907 006	806 651.77	0.01
8- 7	30.747 927	921 799.67	
9- 8	34.587 673	1 036 912.35	
10- 9	38.426 097	1 151 985.40	
11-10	42.263 052	1 267 014.44	
12-11	46.098 393	1 381 995.05	
13-12	49.931 972	1 496 922.86	
14-13	53.763 642	1 611 793.45	
15-14	57.593 258	1 726 602.45	0.02
16-15	61.420 673	1 841 345.45	
17-16	65.245 740	1 956 018.07	
18-17	69.068 313	2 070 615.93	
19-18	72.888 246	2 185 134.63	
20-19	76.705 392	2 299 569.80	-0.11
21-20	80.519 606	2 413 917.05	
22-21	84.330 741	2 528 172.00	
23-22	88.138 651	2 642 330.29	
24-23	91.943 191	2 756 387.53	0.05
25-24	95.744 215	2 870 339.37	
26-25	99.541 578	2 984 181.42	
27-26	103.335 132	3 097 909.33	0.03
28-27	107.124 734	3 211 518.74	
29-28	110.910 238	3 325 005.30	
30-29	114.691 499	3 438 364.63	
31-30	118.468 371	3 551 592.41	
32-31	122.240 710	3 664 684.28	
33-32	126.008 370	3 777 635.90	
34-33	129.771 207	3 891 442.92	-0.02
35-34	133.529 077	4 003 101.02	

(a) The 2σ accuracy of the calculated frequencies increases from ±0.05 MHz for the lower transitions to ±0.10 MHz for the higher (±0.2 to 0.3 $\times 10^{-6}$ cm^{-1}). This uncertainty is the quadrature sum of the error defined by the least square fit, see Table VIII, and the 35 kHz uncertainty of the synthesized frequency as discussed in the text.

III. CO ANALYSIS

The seven measured frequencies of CO were combined with available microwave measured values from the literature for the lower J transitions. The ensemble of experimental values for CO which we used to derive the CO molecular parameters is summarized in Table I. These frequencies were fit to the usual energy expression for the rotational levels of a $^1\Sigma$ diatomic molecule,

$$E(J) = B_0 J(J+1) - D_0 J^2(J+1)^2 + H_0 J^3(J+1)^3 - L_0 J^4(J+1)^4 + M_0 J^5(J+1)^5 + \cdots. \tag{3}$$

(The sign convention here is the same as that used in Ref (7).) The best values for the parameters B_0, D_0, and H_0 were determined by a linear least-squares routine in which the statistical weights were proportional to the inverse squares of the experimental

TABLE III

Observed and Observed − Calculated Frequencies of $H^{37}Cl$ (MHz)

J'-J"	F'-F"	Observed	HFS-corrected Center Freq.	Obs-calc
1-0	3/2-3/2	624 964.374[a]		
	5/2-3/2	624 977.821[a]	624 975.04(0.10)[b]	-0.02
	1/2-3/2	624 988.334[a]		
2-1	5/2-5/2, 3/2-1/2	1 249 558.63		
	5/2-3/2, 7/2-5/2	572.51	1 249 571.39(0.20)	-0.03
	3/2-3/2	582.17		
	1/2-3/2	595.38		
3-2	7/2-7/2	1 873 398.09		
	9/2-7/2, 7/2-5/2	411.28	1 873 410.070(0.20)	-0.02
	5/2-5/2	417.51		
	3/2-3/2	421.31		
4-3	9/2-9/2	2 496 102.07		
	9/2-7/2,11/2-9/2			
	5/2-3/2, 7/2-5/2	114.33	2 496 115.33(0.20)	0.00
	5/2-5/2	127.14		
5-4	11/2-11/2	3 117 295.68		
	13/2-11/2,11/2-9/2			
	9/2-7/2, 7/2-5/2	308.72	3 117 308.72(0.20)	0.03
	7/2-7/2	321.04		
6-5		3 736 615.72	3 736 615.72(0.25)	0.07
7-6		4 353 662.88	4 353 662.88(0.25)	0.04
8-7		4 968 078.97	4 968 078.97(0.30)	-0.07
9-8		5 579 495.42	5 579 495.42(0.30)	-0.11
10-9		6 187 546.55	6 187 546.55(0.40)	0.13

(a) Ref. 6.

(b) The estimated 2σ uncertainty of the experimental measurement is shown in parentheses.

uncertainties. The higher-order terms in this case were not statistically significant and were omitted in the final fit. The derived parameters and their two sigma standard errors (in parentheses) are given in Table VIII. The 35 lowest rotational transitions of CO are calculated and listed in Table II.

IV. HCl ANALYSIS

All the rotational transitions of HCl between 1 and 6 THz ($J + 2 \leftarrow 1$ to $10 \leftarrow 9$) were measured from at least one component of the hyperfine structure (HFS) manifold. The HFS-corrected frequencies together with the previously measured $1 \leftarrow 0$ transitions (*6*) were fit to the energy expression, Eq. (3). In Tables III and IV the observed frequencies, the HFS-corrected center frequencies, and the observed minus calculated frequencies are tabulated for both HCl isotopes; in Tables V and VI, the full HFS spectrum of HCl is tabulated with the uncertainties and HFS modeling defined in

TABLE IV

Observed and Observed − Calculated Frequencies of $H^{35}Cl$ (MHz)

J'-J"	F'-F"	Observed	HFS-Corrected Center Freq.	Obs-Calc
1-0	3/2-3/2	625 901.603[a]		
	5/2-3/2	625 918.756[a]	625 915.20(0.10)[b]	0.03
	1/2-3/2	625 932.007[a]		
2-1	5/2-5/2, 3/2-1/2	1 251 434.34		
	5/2-3/2, 7/2-5/2	451.93	1 251 450.48(0.20)	-0.02
	3/2-3/2	463.91		
	1/2-3/2	480.91		
3-2	7/2-7/2	1 876 210.53		
	5/2-3/2, 3/2-1/2	224.32		
	9/2-7/2, 7/2-5/2	227.50	1 876 226.60(0.20)	0.08
	5/2-5/2	235.41		
	3/2-3/2	240.10		
4-3	9/2-9/2	2 499 847.99		
	9/2-7/2,11/2-9/2 5/2-3/2, 7/2-5/2	864.52	2 499 864.42(0.20)	-0.02
	5/2-5/2	879.86		
5-4	13/2-11/2,11/2-9/2 9/2-7/2, 7/2-5/2	3 121 986.49	3 121 986.49(0.20)	-0.07
6-5		3 742 216.58	3 742 216.58(0.25)	0.02
7-6		4 360 179.99	4 360 179.99(0.25)	-0.05
8-7		4 975 504.67	4 975 504.67(0.30)	0.16
9-8		5 587 820.10	5 587 820.10(0.40)	0.00
10-9		6 196 759.71	6 196 759.71(0.35)	-0.05

(a) Ref. 6.

(b) The estimated 2σ uncertainty of the experimental measurement is shown in parentheses.

TABLE V

Calculated Far-Infrared Transitions of $H^{37}Cl$[a]

J'-J"	F'-F"	MHz	cm^{-1}	Intensity[b] (%)
1-0		624 975.06	20.846 924	
	3/2-3/2	964.37	.846 568	33.3
	5/2-3/2	977.73	.847 013	50.0
	1/2-3/2	988.42	.847 370	16.7
2-1		1 249 571.42	41.681 215	
	3/2-1/2	558.06	.680 770	8.3
	5/2-5/2	559.20	.680 808	9.0
	3/2-5/2	568.75	.681 127	1.0
	1/2-1/2	571.42	.681 216	8.3
	5/2-3/2	572.56	.681 254	21.0
	7/2-5/2	572.56	.681 254	40.0
	3/2-3/2	582.11	.681 572	10.7
	1/2-3/2	595.47	.682 018	1.7
3-2		1 873 410.72	62.490 255	
	7/2-7/2	397.99	.489 831	4.1
	5/2-7/2	404.23	.490 039	0.2
	5/2-3/2	408.05	.490 166	16.0
	3/2-1/2	408.05	.490 166	10.0
	7/2-5/2	411.35	.490 276	24.5
	9/2-7/2	411.36	.490 277	35.7
	5/2-5/2	417.59	.490 484	5.2
	3/2-3/2	421.41	.490 612	4.0
	3/2-5/2	430.96	.490 930	0.3
4-3		2 496 115.33	83.261 445	
	9/2-9/2	102.37	.261 013	2.3
	7/2-9/2	107.06	.261 169	0.07
	7/2-5/2	114.19	.261 407	19.1
	5/2-3/2	114.19	.261 407	14.3
	9/2-7/2	115.73	.261 459	25.5
	11/2-9/2	115.74	.261 459	33.3
	7/2-7/2	120.42	.261 615	3.0
	5/2-5/2	127.56	.261 853	2.3
	5/2-7/2	133.80	.262 061	0.08
5-4		3 117 308.69	103.982 225	
	11/2-11/2	295.59	.981 788	1.5
	9/2-11/2	299.36	.981 914	0.03
	9/2-7/2	308.05	.982 204	20.7
	7/2-5/2	308.06	.982 204	16.7
	11/2-9/2	308.96	.982 234	25.8
	13/2-11/2	308.97	.982 235	31.8
	9/2-9/2	312.74	.982 360	2.0
	7/2-7/2	321.43	.982 650	1.5
	7/2-9/2	326.13	.982 807	0.03

(a) The 2σ uncertainty is ±0.05 MHz (2×10^{-6} cm^{-1}). The HFS shifts were calculated according to eqQ(J) = -53.428 - 0.00387 J(J+1). This is derived using eqQ(1←0) from DeLucia et al.(6) and the J dependence for eqQ($H^{35}Cl$) from Kaiser (11), where we assume that $eqQ = eqQ_o[1+\alpha(B_e/\omega_e)J(J+1)]$. Values of B_e/ω_e are approximated by Y_{01}/Y_{10} from Guelachvili et al.(12), where the relevant reference should be consulted for the symbol definitions.

(b) Relative intensities for the HFS components are defined in Appendix I, Microwave Spectroscopy, C.H. Townes and A.L. Schawlow, p. 499, (Dover, New York, 1975). Brackets identify the Doppler blended components.

TABLE V—*Continued*

J'-J"	F'-F"	MHz	cm^{-1}	Intensity[b] (%)
6-5		3 736 615.65	124.640 082	
	13/2-13/2	602.46	.639 642	1.0
	11/2-13/2	605.62	.639 747	0.01
	11/2-9/2	615.24	.640 068	21.7
	9/2-7/2	615.25	.640 068	18.2
	13/2-11/2	615.84	.640 088	25.9
	15/2-13/2	615.86	.640 089	30.8
	11/2-11/2	619.01	.640 194	1.4
	9/2-9/2	628.63	.640 515	1.0
	9/2-11/2	632.41	.640 641	0.02
7-6		4 353 662.84	145.222 561	
	15/2-15/2	649.59	.222 119	0.8
	13/2-15/2	652.32	.222 210	0.007
	13/2-11/2	662.55	.222 551	22.3
	11/2-9/2	662.57	.222 551	19.2
	15/2-13/2	662.99	.222 566	25.9
	17/2-15/2	663.00	.222 566	30.0
	13/2-13/2	665.72	.222 657	1.0
	11/2-11/2	675.96	.222 998	0.8
	11/2-13/2	679.13	.223 104	0.008
8-7		4 968 079.04	165.717 279	
	17/2-17/2	065.75	.716 836	0.6
	15/2-17/2	068.15	.716 916	0.004
	15/2-13/2	078.83	.717 272	22.8
	13/2-11/2	078.85	.717 273	20.0
	17/2-15/2	079.16	.717 283	29.4
	19/2-17/2	079.17	.717 284	25.9
	15/2-15/2	081.56	.717 363	0.8
	13/2-13/2	092.26	.717 720	0.6
	13/2-15/2	094.99	.717 811	0.005
9-8		5 579 495.53	186.111 938	
	19/2-19/2	482.20	.111 493	0.5
	17/2-19/2	484.34	.111 565	0.003
	17/2-15/2	495.37	.111 932	23.1
	15/2-13/2	495.38	.111 933	20.6
	19/2-17/2	495.62	.111 941	28.9
	21/2-19/2	495.64	.111 942	25.9
	17/2-17/2	497.77	.112 013	0.6
	15/2-15/2	508.81	.112 381	0.5
	15/2-17/2	511.21	.112 461	0.003
10-9		6 187 546.42	206.394 332	
	21/2-21/2	533.05	.393 886	0.4
	19/2-21/2	534.99	.393 951	0.002
	19/2-17/2	546.29	.394 328	23.3
	17/2-15/2	546.31	.394 329	21.1
	21/2-19/2	546.49	.394 335	25.8
	23/2-21/2	546.51	.394 335	28.6
	19/2-19/2	548.43	.394 400	0.5
	17/2-17/2	559.75	.394 777	0.4
	17/2-19/2	561.90	.394 849	0.002
11-10		6 791 869.04	226.552 365	
	23/2-23/2	855.63	.551 918	0.3
	21/2-23/2	857.40	.551 977	0.001
	21/2-19/2	868.93	.552 361	23.5
	19/2-17/2	868.95	.552 362	21.4
	23/2-21/2	869.10	.552 367	25.8
	25/2-23/2	869.12	.552 368	28.3
	21/2-21/2	870.87	.552 426	0.4
	19/2-19/2	882.41	.552 811	0.3
	19/2-21/2	884.35	.552 876	0.001

TABLE VI

Calculated Far-Infrared Transitions of $H^{35}Cl$[a]

J'-J"	F'-F"	MHz	cm^{-1}	Intensity[b] (%)
1-0		625 915.17	20.878 283	
	3/2-3/2	901.65	.877 832	33.3
	5/2-3/2	918.55	.878 396	50.0
	1/2-3/2	932.08	.878 847	16.7
2-1		1 251 450.50	41.743 896	
	3/2-1/2	433.60	.743 332	8.3
	5/2-5/2	435.04	.743 380	9.0
	3/2-5/2	447.12	.743 783	1.0
	1/2-1/2	450.51	.743 896	8.3
	5/2-3/2	451.95	.743 944	21.0
	7/2-5/2	451.95	.743 944	40.0
	3/2-3/2	464.03	.744 347	10.7
	1/2-3/2	480.94	.744 911	1.7
3-2		1 876 226.52	62.584 180	
	7/2-7/2	210.41	.583 643	4.1
	5/2-7/2	218.30	.583 906	0.2
	5/2-3/2	223.13	.584 067	16.0
	3/2-1/2	223.14	.584 068	10.0
	7/2-5/2	227.32	.584 207	24.5
	9/2-7/2	227.33	.584 207	35.7
	5/2-5/2	235.21	.584 470	5.2
	3/2-3/2	240.05	.584 632	4.0
	3/2-5/2	252.13	.585 034	0.3
4-3		2 499 864.44	83.386 502	
	9/2-9/2	848.03	.385 955	2.3
	7/2-9/2	853.96	.386 153	0.07
	7/2-5/2	862.99	.386 454	19.1
	5/2-3/2	863.00	.386 454	14.3
	9/2-7/2	864.95	.386 519	25.5
	11/2-9/2	864.96	.386 519	33.3
	7/2-7/2	870.88	.386 717	3.0
	5/2-5/2	879.91	.387 018	2.3
	5/2-7/2	887.81	.387 282	0.08
5-4		3 121 986.56	104.138 262	
	11/2-11/2	969.98	.137 709	1.5
	9/2-11/2	974.76	.137 869	0.03
	9/2-7/2	985.75	.138 235	20.7
	7/2-5/2	985.76	.138 236	16.7
	11/2-9/2	986.91	.138 274	25.8
	13/2-11/2	986.92	.138 274	31.8
	9/2-9/2	991.69	.138 433	2.0
	7/2-7/2	3 122 002.69	.138 800	1.5
	7/2-9/2	008.63	.138 998	0.03
6-5		3 742 216.60	124.826 910	
	13/2-13/2	199.91	.826 353	1.0
	11/2-13/2	203.92	.826 487	0.01
	11/2-9/2	216.08	.826 892	21.7
	9/2-7/2	216.10	.826 893	18.2
	13/2-11/2	216.85	.826 918	25.9
	15/2-13/2	216.87	.826 918	30.8
	11/2-11/2	220.86	.827 052	1.4
	9/2-9/2	233.04	.827 458	1.0
	9/2-11/2	237.81	.827 617	0.02

(a) The 2 σ uncertainty is ± 0.05 MHz ($\pm 2 \times 10^{-6}$ cm^{-1}). The HFS shifts are calculated using the results of Kaiser (11).

(b) Relative intensities for the HFS components are defined in Appendix I, p. 499, Microwave Spectroscopy, C.H. Townes and A.L. Schawlow, (Dover, New York, 1975). Brackets identify the Doppler blended components.

TABLE VI—*Continued*

J'-J"	F'-F"	MHz	cm^{-1}	Intensity[b] (%)
7-6		4 360 180.04	145.439 951	
	15/2-15/2	163.28	.439 392	0.8
	13/2-15/2	166.73	.439 507	0.007
	13/2-11/2	179.68	.439 939	22.3
	11/2-9/2	179.70	.439 940	19.2
	15/2-13/2	180.23	.439 957	25.9
	17/2-15/2	180.25	.439 958	30.0
	13/2-13/2	183.69	.440 073	1.0
	11/2-11/2	196.65	.440 505	0.8
	11/2-13/2	200.66	.440 639	0.008
8-7		4 975 504.51	165.964 966	
	17/2-17/2	487.68	.964 405	0.6
	15/2-17/2	490.72	.964 506	0.004
	15/2-13/2	504.24	.964 957	22.8
	13/2-11/2	504.26	.964 958	20.0
	17/2-15/2	504.65	.964 971	29.4
	19/2-17/2	504.67	.964 971	25.9
	15/2-15/2	507.69	.965 072	0.8
	13/2-13/2	521.23	.965 524	0.6
	13/2-15/2	524.68	.965 639	0.005
9-8		5 587 820.10	186.389 615	
	19/2-19/2	803.22	.389 053	0.5
	17/2-19/2	805.94	.389 143	0.003
	17/2-15/2	819.89	.389 608	23.1
	15/2-13/2	819.91	.389 609	20.6
	19/2-17/2	820.21	.389 619	28.9
	21/2-19/2	820.23	.389 620	25.9
	17/2-17/2	822.93	.389 710	0.6
	15/2-15/2	836.90	.390 176	0.5
	15/2-17/2	839.94	.390 277	0.003
10-9		6 196 759.76	206.701 656	
	21/2-21/2	742.84	.701 092	0.4
	19/2-21/2	745.29	.701 174	0.002
	19/2-17/2	759.59	.701 651	23.3
	17/2-15/2	759.61	.701 651	21.1
	21/2-19/2	759.85	.701 659	25.8
	23/2-21/2	759.87	.701 660	28.6
	19/2-19/2	762.30	.701 741	0.5
	17/2-17/2	776.62	.702 219	0.4
	17/2-19/2	779.34	.702 309	0.002
11-10		6 801 959.63	226.888 951	
	23/2-23/2	942.67	.888 385	0.3
	21/2-23/2	944.91	.888 460	0.001
	21/2-19/2	959.49	.888 946	23.5
	19/2-17/2	959.52	.888 947	21.4
	23/2-21/2	959.70	.888 953	25.8
	25/2-23/2	958.73	.888 954	28.3
	21/2-21/2	961.95	.889 028	0.4
	19/2-19/2	976.55	.889 516	0.3
	19/2-21/2	979.01	.889 597	0.001

appropriate footnotes. In Table VIII the molecular parameters obtained by the fitting procedure and used for the calculated lines are summarized.

V. HF ANALYSIS

In Table VII we show the differences between the observed minus calculated frequencies for the five lowest rotational transitions of HF which fall in the FIR range. For the calculated frequencies we use the model parameters (see Table VIII) based

TABLE VII

Calculated and Observed − Calculated HF Rotational Frequencies[a]

J'-J"	Calculated Frequency in units of: cm^{-1}	MHz	Obs-calc (MHz)
1-0	41.110 9816(46)[b]	1 232 476.22(14)	0.05
2-1	82.171 1168(71)	2 463 428.11(21)	0.03
3-2	123.129 6765(95)	3 691 334.84(28)	-0.19
4-3	163.936 166(20)	4 914 682.61(62)	-0.04
5-4	204.540 440(44)	6 131 968.10(130)	0.30

(a) Calculated frequencies are from Ref. 1 in which the fit is based on a total of 18 measured lines, including those listed here.

(b) The 2σ uncertainties, shown in parentheses, apply to the least significant digits.

upon a larger set of measurements obtained in a complementary study to this work (7). Reference (7) should be consulted for the details of the HF model fit.

VI. CONCLUSIONS

We have used new techniques for producing tunable FIR radiation to provide a comprehensive set of accurately measured transitions of gases which can serve as

TABLE VIII

Ground State Molecular Constants for CO, HCl, and HF (MHz)

Coef.	CO	$H^{37}Cl$	$H^{35}Cl$	HF[a]
B_o	57 635.9660(34)[b]	312 519.0954(126)	312 989.2443(154)	616 365.199(75)
D_o	0.183 5053(58)	15.783 33(27)	15.830 50(32)	63.5532(41)
H_o	$1.731(15)\times10^{-7}$	$4.947(16)\times10^{-4}$	$4.931(19)\times10^{-4}$	$4.897(15)\times10^{-3}$
L_o	---	---	---	$4.41(20)\times10^{-7}$
M_o	---	---	---	$2.82(80)\times10^{-11}$
No. Data in Fit	12	10	10	18

(a) The HF values are from Ref. 1.

(b) The 2σ uncertainties, shown in parentheses, were obtained from the statistical fit and refer to the least significant digits.

highly accurate spectroscopic standards. The accuracy of the derived frequencies is better than one part in 10^7. The use of the spectra of these molecules for calibration should improve the accuracy in high-resolution spectroscopy and may aid in the astrophysical observations of their molecular transitions.

ACKNOWLEDGMENTS

This project was initiated with an NSF International Studies grant (US-Italian Program) at the University of Oregon (NSF 81-18513), and carried to completion with additional support by NASA (NAGW-222) and Murdock Foundation grants; and supported at NBS by NASA contract W15,047. Research at the Smithsonian Astrophysical Observatory was supported by the Chemical Manufacturers Association (FC85-544). G.D.L. acknowledges the support of the Consiglio Nazionale delle Ricerche; K.R.L. the support of an NRC Associateship; and A.H. the support of the Deutsche Forschungsgemeinshaft. J. E. Davis and S. Predko provided valuable support with detector systems, and J. Hardwick verified some of the fitting algorithms.

RECEIVED: March 12, 1987

REFERENCES

1. P. HELMINGER, J. K. MESSER, AND F. C. DE LUCIA, *Appl. Phys. Lett.* **42,** 309–310 (1983).
2. R. L. POYNTER AND H. M. PICKETT, private communication; P. HELMINGER, J. K. MESSER, W. C. BOWMAN, AND F. C. DELUCIA, *J. Quant. Spectrosc. Radiat. Transfer* **32,** 325–333 (1984).
3. J. W. C. JOHNS, *J. Opt. Soc. Amer. B* **2,** 1340–1354 (1985).
4. K. M. EVENSON, D. A. JENNINGS, AND F. R. PETERSON, *J. Appl. Phys.* **44**(6), 576–578 (1984).
5. F. R. PETERSON, E. C. BEATY, AND C. R. POLLOCK, *J. Mol. Spectrosc.* **102,** 112–122 (1983); L. C. BRADLEY, K. L. SOOHOO, AND C. FREED, *IEEE J. Quantum Electron.* **22,** 234–267 (1986).
6. F. C. DE LUCIA, P. HELMINGER, AND W. GORDY, *Phys. Rev. A* **3,** 1849–1857 (1971).
7. D. A. JENNINGS, K. M. EVENSON, L. R. ZINK, C. DEMUYNCK, J. L. DESTOMBES, B. LEMOINE, AND J. W. C. JOHNS, *J. Mol. Spectrosc.* **122,** 477–480 (1987).
8. B. ROSENBLUM, A. H. NETHERCOT, AND C. H. TOWNES, *Phys. Rev. A* **109,** 400–412 (1958).
9. W. GORDY AND M. J. COHEN, *Bull. Amer. Phys. Soc.* **2,** 212 (1957).
10. P. HELMINGER, F. C. DE LUCIA, AND W. GORDY, *Phys. Rev. Lett.* **25,** 1397–1399 (1970).
11. E. W. KAISER, *J. Chem. Phys.* **53,** 1686–1703 (1970).
12. G. GUELACHVILI, P. NIAY, AND P. BERNAGE, *J. Mol. Spectrosc.* **85,** 271–281 (1981); G. GUELACHVILI, *Opt. Commun.* **19,** 150–154 (1976).